

## Comprehensive GRAPPA

J. Miao<sup>1</sup>, W. C. Wong<sup>1,2</sup>, D. Huo<sup>3</sup>, and D. L. Wilson<sup>1,4</sup>

<sup>1</sup>Biomedical Engineering, Case Western Reserve University, Cleveland, Ohio, United States, <sup>2</sup>Computer Science and Engineering, The Hong Kong University of Science and Technology, Kowloon, Hong Kong, <sup>3</sup>Keller Center for Imaging Innovation, St. Joseph Hospital and Medical Center, Phoenix, Arizona, United States,

<sup>4</sup>Radiology, University Hospitals of Cleveland, Cleveland, Ohio, United States

**INTRODUCTION** Synthesizing unsampled signal from sampled signals is an ultimate goal in parallel MR k-space reconstruction. Most algorithms like GRAPPA [1] achieve the reconstruction with global linear regression (GLR). They all make a common assumption that unsampled signals can be explained linearly and globally by sampled one. Theoretically, we reveal that the relationship between missing and sampled data is correlated to coil sensitivity and noise and, therefore, the global assumption is invalid. To better model such relationship, we locally fit the linear function within subregions on a mathematically sound framework, Geographically Weighted Regression (GWR) [2]. Instead of using a single set of complex weights for the reconstruction, this novel approach uses multiple sets. Extra computation efforts for the partitioning and addition calibration in this new algorithm are negligible. Over 1000 images of simulated and acquired MR data with different image contents and different acquisition schemes including MR tagging data were tested. A perceptual difference model (Case-PDM) [3] was used to quantitatively evaluate the image quality and to optimize the parameters of the new algorithm.

**THEORY AND METHODS** Solving the complex weights is an ill-posed problem. GRAPPA adopts the Moore-Penrose pseudo-inverse to find a partial solution,  $\hat{n}_j^m \approx (S_m^T S_m)^{-1} S_m^T \hat{s}_j^{\text{ACS}}$  (1), where  $\hat{n}_j^m$  is a column vector whose elements denoting complex weights for the  $j^{\text{th}}$  coil and  $m^{\text{th}}$  missing line ( $j \in [1, L]$ ,  $L$  is the number of coils;  $m \in [1, A-1]$ ,  $A$  is the accelerating factor),  $\hat{s}_j^{\text{ACS}}$  is a column vector whose elements enumerating the ACS signals,  $S_m$  is a matrix that tabulates ACS data covered by the sliding complex weights kernel. This procedure is equivalent to GLR on the ACS signals. It implies the original GRAPPA reconstruction assumes a single set of complex weights is sufficient. To better understand the theoretical meaning of the complex weights, we have derived their relationship to coil sensitivity data by the convolution theorem. From the study, we found that the complex weights are correlated to both coil sensitivity and noise. Therefore, they should not be constant over the k-space and are non-stationary. We suggest the complex weights should be localized—varied with the acquired k-space data—according to the spatial analysis theory [4]. This leads to the development of the novel comprehensive GRAPPA reconstruction algorithm. We introduced GWR, an adequate framework to deal with spatial non-stationarity, to GRAPPA. On the GWR framework, complex weights are continuous functions in a space  $\Omega$ . The  $\Omega$  space is defined by a  $1 \times L$  vector  $\bar{\mu}_{i,m}$  whose  $i^{\text{th}}$  element is the average signal magnitude within the kernel acquired by the  $i^{\text{th}}$  coil and where  $i$  denotes location. To reflect this change, Eq. (1) is rewritten to  $\hat{n}_j^m(i) \approx (S_m^T \mathbf{W}_m(i) S_m)^{-1} S_m^T \mathbf{W}_m(i) \hat{s}_j^{\text{ACS}}$  (2), where  $\mathbf{W}_m(i)$  is a diagonal matrix containing locality weights that help model the underlying non-stationarity. Elements of  $\mathbf{W}_m(i)$  are normalized inverse distance between  $\bar{\mu}_{i,m}$  and those  $\mu$  of the acquired ACS signals. Regarding the reconstruction of missing signal at  $(k_x, k_y, l, m)$ , we calculate  $\mu$  at  $(k_x, k_y, l, m)$  and the diagonal matrix  $\mathbf{W}_m$  at  $(k_x, k_y, l, m)$ , then we obtain the complex weights with Eq. (2). As a final step, we reconstruct the missing data in a way identical to original GRAPPA. Our algorithm can be speeded by partitioning  $\Omega$  space into  $P$  clusters with k-means algorithm. The index  $i$  in Eq. (2) is changed to  $p$  denoting the complex weight computation of the  $p^{\text{th}}$  cluster.

Our algorithm was tested with both phantom and *in vivo* MR data of different image contents and different acquisition schemes (including MR tagging data). We also investigated the important factors that affect the optimal number of clusters  $P_{\text{best}}$  based upon Case-PDM.

**RESULTS** To demonstrate the robustness of our algorithm, all MR images were reconstructed without any ACS integrated into final reconstructions, even in some cases where combinable ACS were available. Experimental results showed that Comprehensive GRAPPA with 2 clusters  $P = 2$  gave reconstruction with significantly better image quality than the original algorithm, by both PDM score and visual inspection in all head-to-head comparisons amongst all test images. More clusters ( $P > 2$ ) used will produce higher image quality until it saturates at  $P = P_{\text{best}}$ . Simulation results show that the  $P_{\text{best}}$  is dependent on the number of coil elements, type of imaged object and sampling conditions, but not on the coil sensitivity and noise level.

**CONCLUSION** The proposed comprehensive GRAPPA reconstruction algorithm with GWR is a generalization of GLR-based GRAPPA. With a single cluster, our algorithm reduces to the original implementation. We found that a few clusters (say, 2) are sufficient enough to give significantly better reconstruction than the original GRAPPA in terms of image quality. From the simulation, we know that there are three factors that affect the optimal number of clusters used in the algorithm. They are imaged object type, number of channels and acceleration factor. Although there may not have a universal optimal number of clusters, one can optimize it according to scanning protocols for clinical imaging in which those factors are invariant. If optimization is not possible, as a rule of thumb, we suggest using at least two clusters for the reconstruction. Case-PDM, an objective measure to quantify human perception on image quality, is an invaluable metric in this work; we used it to optimize MR reconstruction parameters and determine the dependent factors of the optimal cluster number. Moreover, accuracy of GWR can be boosted with filtering local outliers [5] and other regularization methods [6] that are developed for GLR. We expect that the proposed novel reconstruction framework can be extended to other parallel image reconstruction algorithms such as SENSE, SMASH and PARS. Also, our algorithm is ready for dynamic MR imaging, especially cardiac MR imaging with spin tagging.

**ACKNOWLEDGEMENT:** This work was supported under NIH grant R01 EB004070 and the Research Facilities Improvement Program Grant NIH C06RR12463-01. We thank Mark A. Griswold for helpful discussion and Martin Blaimer for his generous help in the acquisition of some of parallel MR data used in this work.

**REFERENCES:** [1] Griswold et al., MRM 2002 [2] Fotheringham et al., John Wiley & Sons Press [3] Miao et al., Med. Phys. 2008 [4] Fortin et al., Cambridge University Press [5] Huo et al., JMRI 2008 [6] Qu et al., JMRI 2006

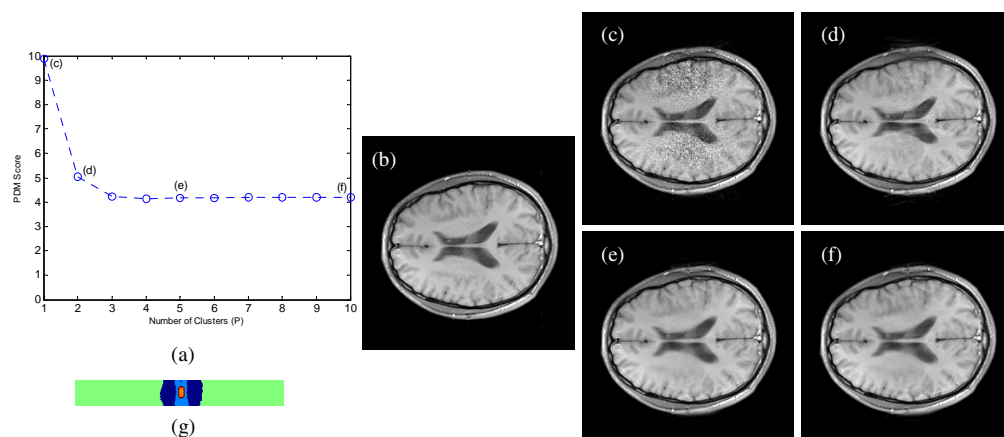


**Figure** Algorithm demonstration for a 4-channel MR brain data set (full-sampled data size =  $256 \times 256 \times 4$ ). For the undersampled data (AF = 3, ACS = 30), more clusters used can improve image quality of GRAPPA reconstruction until the image quality saturates at  $P = 5$ , as demonstrated by a result in (a). Letters above the circles correspond to images reconstructed from the same data with different number of clusters. (b) is a reference image created from full k-space data with a PDM score of zero. Original GRAPPA is in the case of one cluster. (g) demonstrates the partitioned  $\Omega$  space of ACS with different color denoting each of the 5 clusters.